Organic & Biomolecular Chemistry

ROYAL SOCIETY OF CHEMISTRY

PAPER

View Article Online
View Journal | View Issue

Cite this: *Org. Biomol. Chem.*, 2021, **19**, 1133

$PhI(OAc)_2$ and iodine-mediated synthesis of *N*-alkyl sulfonamides derived from polycyclic aromatic hydrocarbon scaffolds and determination of their antibacterial and cytotoxic activities†

Megan D. Hopkins, Garett L. Ozmer, Ryan C. Witt, Zachary C. Brandeburg, David A. Rogers, Claire E. Keating, Presley L. Petcoff, Robert J. Sheaff* and Angus A. Lamar *

The development of new approaches toward chemo- and regioselective functionalization of polycyclic aromatic hydrocarbon (PAH) scaffolds will provide opportunities for the synthesis of novel biologically active small molecules that exploit the high degree of lipophilicity imparted by the PAH unit. Herein, we report a new synthetic method for C–X bond substitution that is speculated to operate *via* a N-centered radical (NCR) mechanism according to experimental observations. A series of PAH sulfonamides have been synthesized and their biological activity has been evaluated against Gram-negative and Gram-positive bacterial strains (using a BacTiter-Glo assay) along with a series of mammalian cell lines (using CellTiter-Blue and CellTiter-Glo assays). The viability assays have resulted in the discovery of a number of bactericidal compounds that exhibit potency similar to other well-known antibacterials such as kanamycin and tetracycline, along with the discovery of a luciferase inhibitor. Additionally, the physicochemical and drug-likeness properties of the compounds were determined experimentally and using *in silico* approaches and the results are presented and discussed within.

Received 3rd December 2020,
Accepted 7th January 2021

DOI: 10.1039/d0ob02429e

rsc.li/obc

Introduction

Due to the indiscriminate use of antimicrobial agents and a relatively slow developmental pace of new antibacterial agents, the emergence of drug-resistant bacterial infections has been listed by the World Health Organization as one of the top 10 health threats in the world.[1] The search for novel chemotherapeutics and/or new antibacterial mechanisms for treating drug-resistant bacterial infections is therefore an urgent need amongst the scientific community. In general, multi-drug resistant bacterial cells are able to repel current chemotherapeutic agents through one of the following mechanisms: (1) enzymatic destruction of the antibiotic; (2) reduction in cell membrane permeability; (3) efflux pumps; and (4) modification of the drug target site.[2] Targeting or disrupting the bacterial cell membrane is an approach that can circumvent many of the bacterial resistance mechanisms, and recent advances have been made in the classes of polymyxins (colistin and polymyxide B), β-lactams (cefiderocol), and peptide mimetics (murepavadin) to treat multi-drug resistant Gram-negative bacterial infections.[3] It has recently been reported that fluorenylmethyloxycarbonyl (Fmoc)-conjugated amino acids and peptides demonstrate considerable antimicrobial activity.[4] It is believed that the potency of the bacterial inhibition is directly related to the hydrophobic nature of the amino acid side chains and lipophilicity of the fluorenyl portion of the Fmoc group.[4] Although the exact nature of the mode of action is unknown, it is believed that the amphipathic Fmoc-amino acid compounds target bacterial membranes in a surfactant-like behavior.[4] Investigation of fluorene as a lipophilic, polycyclic aromatic hydrocarbon (PAH) scaffold in the development of bioactive small molecules as potential antibacterial agents is a desirable pursuit that has the potential to lead to new areas of research in medicinal chemistry.

Polycyclic aromatic hydrocarbons have a variety of applications, including use as light-emitting devices, organic transistors, biosensors, and organic photovoltaic cells, among others.[5] Fluorene, one of the simplest PAH cores, is a rigid, planar biphenyl core that has been observed as a substructure within a variety of bioactive molecules, most notably when substituted with a nitrogen-containing functionality at the 9-position (Fig. 1).[4,6]

Department of Chemistry and Biochemistry, The University of Tulsa, 800 South Tucker Drive, Tulsa, Oklahoma, 74104, USA. E-mail: angus-lamar@utulsa.edu

†Electronic supplementary information (ESI) available. See DOI: 10.1039/d0ob02429e

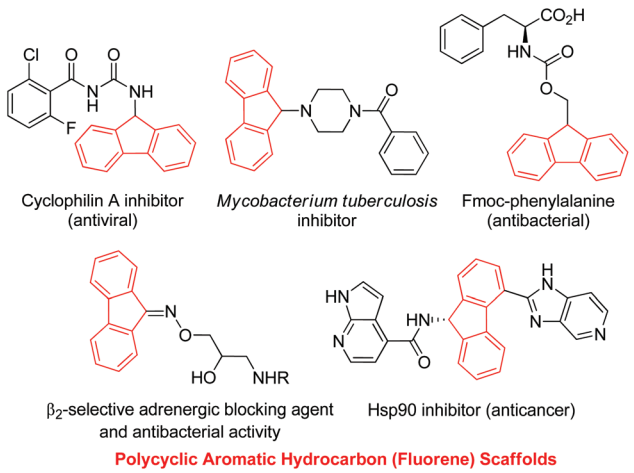

Fig. 1 Selected examples of pharmaceuticals and bioactive compounds that contain polycyclic aromatic hydrocarbon (PAH) scaffolds. The fluorene core is shown in red.

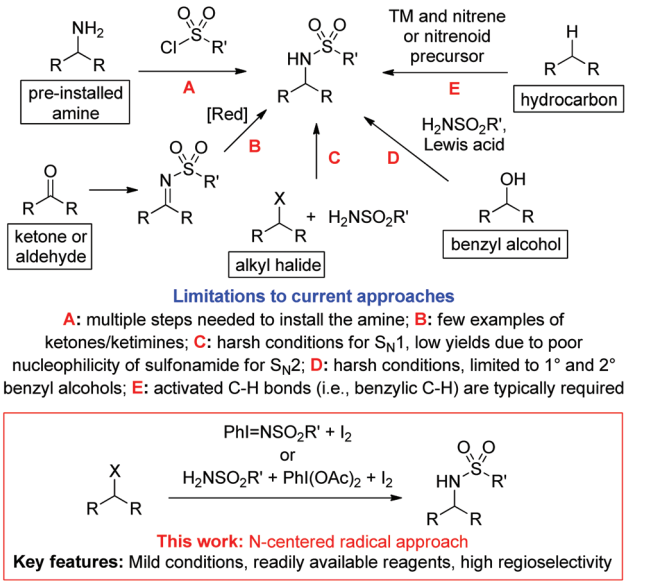

Scheme 1 Current approaches for installation of a *N*-alkyl sulfonamide unit to a hydrocarbon core.

The majority of PAH-containing bioactive molecules take advantage of lipophilic properties imparted by the hydrocarbon core to engage central nervous system (CNS) and/or neurological targets.[7] Inspired by the notable examples of bioactive compounds containing a fluorene core with amino-substitution at the 9-position shown in Fig. 1, and following our interest in the development of new methods for sulfonamide insertion,[8–11] we aimed to generate sulfonamide analogs from commercially available halogenated PAH scaffolds to test for biological activity.

Sulfonamides are an important bioisosteric functionality within the science of drug discovery and development, as evidenced by the number of pharmaceutical and bioactive compounds that contain a sulfonamide unit.[12] As a class of therapeutic agent, sulfonamides have displayed a broad pharmacological profile that includes anti-inflammatory, antiparasitic, antibacterial, antithyroid, antiviral, hypoglycemic, diuretic, and anticancer activities.[13] Despite having a plethora of options for the installation of a sulfonamide moiety to a hydrocarbon substrate,[14] synthetic limitations still exist that warrant the development of new approaches. Current methods to directly install a sulfonamide unit into a molecular scaffold include: (A) reaction of pre-installed amines with sulfonyl chlorides (Scheme 1A);[15] (B) reduction of *N*-sulfonyl imines formed from carbonyl-containing precursors (Scheme 1B);[16] (C) alkyl halides reacting with nucleophilic sulfonamides (Scheme 1C);[16] (D) Lewis-acid catalyzed *N*-sulfonamidation of 1° and 2° benzylic alcohols (Scheme 1D);[16] (E) benzylic C–H activation using transition-metals or nitrene precursors (Scheme 1E);[16] (F) oxidation of sulfinimides;[17] or (G) oxidative coupling between sulfinate salts and amines.[18] Recently, our lab developed a synthetic method to incorporate *N*-sulfonyl units into 3° (sp^3) C–X positions under ambient conditions (20 °C) to form α-tertiary amines.[8] According to mechanistic investigations, the reaction is speculated to operate through a nitrogen-centered radical (NCR)[19] precursor, *N*,*N*-diiodosulfonamide, formed *in situ* under visible-light conditions from an iminoiodinane reagent (PhI=NSO_2R) and molecular iodine.[8] We envisioned that a NCR approach could also be applied to sterically hindered 2° (sp^3) halogenated PAH substrates in order to directly produce a wide variety of *N*-sulfonylamino analogs from hydrocarbon scaffolds under mild, operationally simple conditions.

The synthesis of 9-aminosulfonylfluorene derivatives have been reported from intramolecular Aza-Friedel–Crafts reaction pathways using 2-formyl biphenyl substrates in the presence of a Lewis acid catalyst,[20] albeit with relatively limited scope of sulfonamide substrate. In addition, C–H activation approaches have been reported, but with limited scope and/or modest yields.[21] More recently, examples of 9-aminofluorene derivatives have been reported using a Pd-catalyzed cross-coupling/annulation pathway,[22] however, sulfonamide was not employed as a *N*-substrate. The direct, non-metal promoted installation of a wide range of sulfonamide units into a 2° C–X bond using a commercially available, air-stable oxidant (PhI$(OAc)_2$) and I_2 provides a new method for forming sulfonamides from PAH scaffolds. Herein we report the development of a practical reaction to add to the synthetic toolkit for regioselective functionalization of PAH scaffolds along with the creation of an initial library of *N*-alkyl sulfonamides to screen for biological activity.

Results and discussion

Synthesis of PAH sulfonamide library compounds 2–23

To begin our investigation, we selected 9-bromofluorene as a representative PAH scaffold. Our initial attempt to activate 9-bromofluorene **1** for *N*-sulfonamide substitution under a

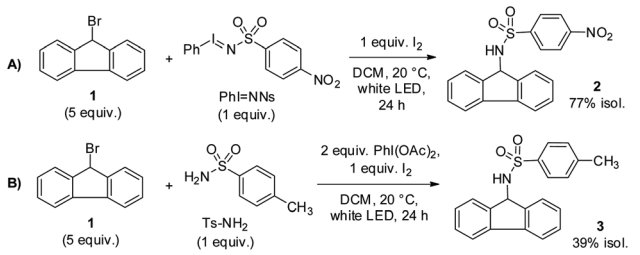

Scheme 2 Initial attempt to form 9-aminosulfonyl products from 9-bromofluorene.

visible-light-promoted, radical pathway using an iminoiodinane (PhI=NNs) resulted in formation of **2** in good yield (Scheme 2A). Stoichiometry and reaction conditions were based upon our earlier report of 3° C–X activation. Although iminoiodinane reagents have proven to be valuable *N*-sources for C–N bond-forming NCR reactions, the requirement to preform the reagent and store at low temperatures limits the practicality of the approach. In order to circumvent the use of a pre-formed iminoiodinane reagent, an additional experiment was conducted to determine if the production of **3** could result from the use of commercially available, temperature stable reagents such as molecular iodine, $PhI(OAc)_2$ and a *N*-sulfonamide. To our delight, a moderate yield of **3** was obtained (Scheme 2B) indicating that a more convenient reaction than our previous $PhI{=}NSO_2R/I_2$ system could potentially be established.

The optimization of reaction conditions using 9-bromofluorene **1** and a $PhI(OAc)_2/I_2$/*N*-sulfonamide system is shown in Table 1. Dichloromethane was determined to be the optimal solvent (entries 1–5). At room temperature, the yield of **3** was limited to 47% yield and was not improved by using an excess of **1** (entries 5 and 6). When heated to 50 °C, the reaction performed with similar efficiency (entries 5 and 7), however, stoichiometric modifications resulted in a dramatically improved yield of **3** (entries 7–9). When using 2–5 equivalents of **1**, the best results were obtained from allowing the reaction to proceed for 24 hours (entries 8, 10 and 11). Further stoichiometric modifications were attempted (entries 12–14), though substantial improvements beyond entry 8 were not observed. Thus, the optimized reaction conditions are as follows: 2 equivalents **1**, 1 equiv. *N*-sulfonamide, 1 equiv. I_2, in CH_2Cl_2 at 50 °C for 24 hours.

In order to verify that the $PhI(OAc)_2/I_2$/*N*-sulfonamide system is operating through the hypothesized NCR-mediated radical pathway, the following control/mechanistic experiments were conducted (Table 2). When using 9-chlorofluorene as alkyl halide substrate (Table 2, entry 2), the reaction resulted in a decreased yield, analogous to the previously reported study using 3° alkyl halides.[8] This result offers indirect evidence regarding the ease of homolytic C–X bond cleavage by an NCR species based upon C–X bond strengths. In the absence of I_2, the reaction proceeds with drastically reduced efficiency (entry 3). Similarly, when $PhI(OAc)_2$ is excluded, a reduction in the yield of **3** is also observed (entry 4). When both I_2 and $PhI(OAc)_2$ are excluded (entry 5), the reaction is completely halted. This indicates that sulfonamide will not act as a nucleophile in S_N2-type mechanism with 9-bromofluorene under the reaction conditions, nor will 9-bromofluorene undergo S_N1-type substitution at 50 °C. Lastly, a known radical inhibitor, 2,2,6,6-tetramethyl-1-piperidinyloxy (TEMPO), was added to the standard reaction conditions, and the formation of product **3** was drastically reduced (entry 6). Attempts to isolate a TEMPO-fluorene adduct were unsuccessful, however evidence of trace amount of the adduct was observed by MS. The attenuated yield of **3** provides additional

Table 1 Optimization of stoichiometry and reaction conditions

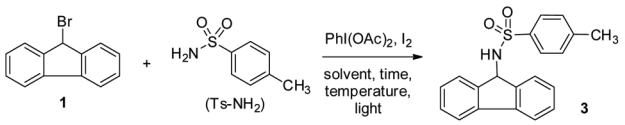

Entry	Equiv. **1**	Equiv. Ts-NH_2	Equiv. $PhI(OAc)_2$	Equiv. I_2	Solvent	Temp. (°C)	Time (h)	Light (LED)	Yield **3**[a] (%)
1	1	1	2	1	$CHCl_3$	20	24	White	35
2	1	1	2	1	DCE	20	24	White	20
3	1	1	2	1	Et_2O	20	24	White	6
4	1	1	2	1	THF	20	24	White	13
5	1	1	2	1	CH_2Cl_2	20	24	White	47
6	5	1	2	1	CH_2Cl_2	20	24	White	39
7	1	1	2	1	CH_2Cl_2	50	24	—	46
8	2	1	2	1	CH_2Cl_2	50	24	—	83
9	5	1	2	1	CH_2Cl_2	50	24	—	85
10	5	1	2	1	CH_2Cl_2	50	8	—	80
11	2	1	2	1	CH_2Cl_2	50	8	—	62
12	5	1	2	0.2	CH_2Cl_2	50	24	—	31
13	1	2	2	1	CH_2Cl_2	50	24	—	58
14	2	1	1	1	CH_2Cl_2	50	24	—	65

[a] All yields are isolated.

Table 2 Mechanistic/control experiments

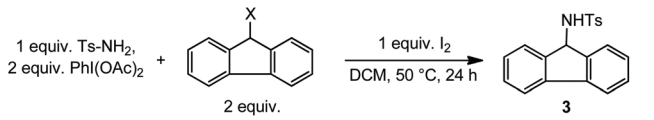

Entry	X	Deviation from standard conditions	% 3[a]
1	Br	No deviation	83
2	Cl	No deviation	33
3	Br	0 equiv. I_2	20
4	Br	0 equiv. $PhI(OAc)_2$	22
5	Br	0 equiv. I_2, 0 equiv. $PhI(OAc)_2$	0
6	Br	1 equiv. TEMPO added	10

[a] All yields are isolated.

indirect evidence for the formation of a benzylic radical that is generated by activation from the $PhI(OAc)_2/I_2$/*N*-sulfonamide system *via in situ* formation of the NCR precursor, *N*,*N*-diiodosulfonamide.

A mechanistic pathway is proposed in Scheme 3 on the basis of literature reports of related systems and the experimental observations described in Table 2.[8,23] Upon generation of *N*-iodosulfonamide species **A**, the labile N–I bond undergoes homolytic cleavage in the presence of ambient light or heat to form N-centered radical species **B** and iodine radical. Abstraction of the bromine from the representative 9-bromofluorene is most likely facilitated by the liberated iodine radical to form a relatively stable benzylic radical at the 9-position of fluorene (species **C**). The stabilized carbon radical species can then combine with the N-centered radical **B** to directly form the 9-aminosulfonylfluorene product **E** or abstract an iodine atom (from either I_2, species **A**, AcOI, or I–Br) to form a highly reactive 9-iodofluorene intermediate **D**. Species **D** would be more susceptible than 9-bromofluorene to nucleophilic attack from a sulfonamide (with release of HI), and could undergo reaction to form product **E**. Evidence of the benzylic radical species **C** is supported by observation of trace amounts of trapped species **F** and **G** by MS.

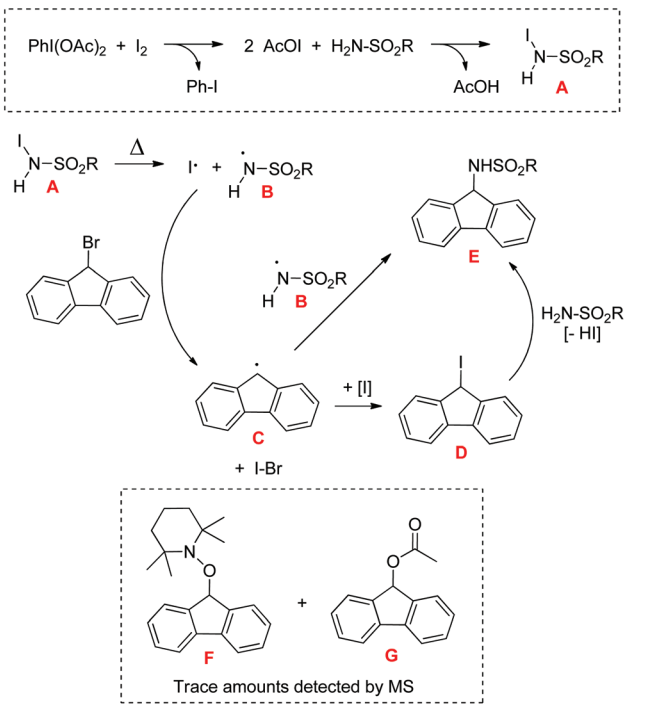

Scheme 3 Plausible mechanism for $PhI(OAc)_2$ and I_2-mediated synthesis of 9-aminosulfonylfluorene compounds.

With an optimized set of reaction conditions, the scope of the *N*-sulfonamide reagent was explored (Fig. 2). A variety of 4-substituted aryl sulfonamides were tested, and yields were consistently moderate to good (Fig. 2, products **2**–**7**). Compound **5** was prepared in gram scale (1.2 g isolated) without a decrease in efficiency. The use of electron deficient 3-substituted aryl sulfonamides, however, resulted in lower yields (**9**–**11**) when compared to analogous 4-substituted or 2-substituted aryl sulfonamide substrates. A notable exception to this trend was observed from the use of 3,5-difluorobenzenesulfonamide, which resulted in an acceptable 54% yield of product **16**. Utilization of the majority of 2-substituted aryl sulfonamides resulted in moderate yields ranging from 44–74% (**12**–**15**, and **17**–**18**). An alkyl sulfonamide was also shown to be a viable reacting partner, resulting in product **19**. In addition to 9-bromofluorene, 2,9-dibromofluorene was employed to produce **20**, albeit in low yield which we suspect is a result of

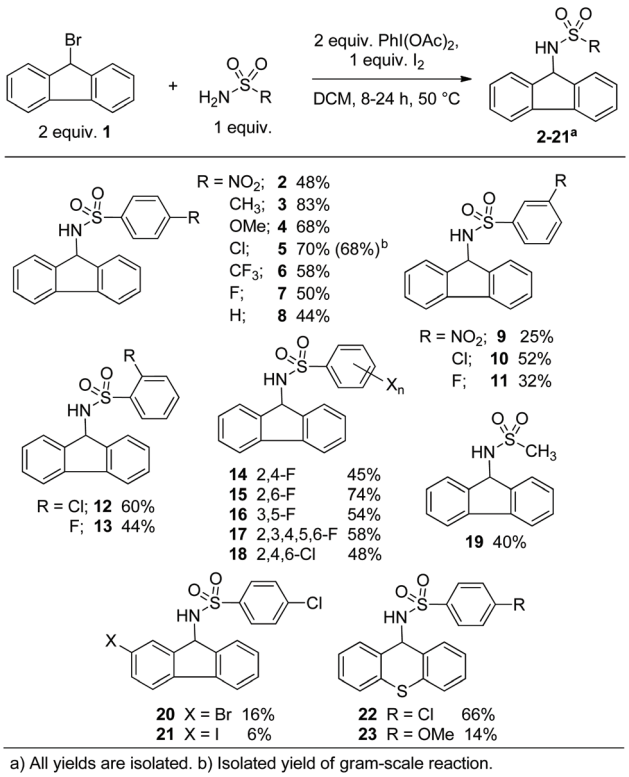

Fig. 2 Substrate scope of 9-aminosulfonyl fluorene and heteroanthracene products. [a]All yields are isolated. [b]Isolated yield of gram-scale reaction.

poor solubility, with selectivity for *N*-substitution occurring exclusively at the 9-Br position. Lastly, a 9-bromo-9*H*-thioxanthene substrate, prepared from thioxanthen-9-one, was tested as a representative 9-bromoheteroanthracene substrate, resulting in a 66% yield of **22**.

In vitro antibacterial screening of 2–23

To test the bactericidal effects of the library compounds, representative Gram-positive and Gram-negative bacterial strains were selected for screening. An initial bacterial cell viability screening of library compounds (50 μM) against *Staphylococcus aureas* (MicroKwik Culture from Carolina), a Gram-positive bacteria, was conducted using BacTiter-Glo Cell Viability (Promega) assay, which is an assay that measures cell viability by indirectly measuring a protease released by dying cells that cleaves a peptide conjugated to firefly luciferin. The released luciferin is oxidized to luciferase, releasing light which can be correlated with the number of dead cells. The bacterial cells were treated with library compounds at 50 μM concentration for 8 hours, and none of the compounds displayed considerable activity relative to the DMSO background. The concentration was adjusted to 500 μM and compounds **17** and **23** demonstrated activity comparable to known antibacterials kanamycin and tetracycline (Fig. 3).

In a separate control reaction performed (based upon literature precedent)[11,24] in which exogenous ATP was added to media in the absence of cells, it was confirmed that compounds **2**–**22** (50 μM, 10 min exposure) do not inhibit the CellTiter-Glo luciferase assay itself (CellTiter-Glo is similar to BacTiter-Glo but without a buffer to lyse bacterial cells). However, compound **23** displayed substantial activity as a luciferase inhibitor (Fig. 4) and this effect may account for the activity displayed against *S. aureas* at 500 μM. Due to the use of luciferase in reporter systems, there is interest in the scientific community in understanding luciferase activity and its regulation.[25] The development of new small molecules that block luciferase activity has been a topic of pursuit,[24,26] and further study of compound **23** as a luciferase inhibitor is warranted.

A bacterial cell viability screening of library compounds (50 μM; approximately 15–20 μg mL^{-1}) against *E. coli* (JM109 strain), a representative Gram-negative bacteria, was also conducted using BacTiter-Glo Cell Viability (Promega) assay. Compounds **2**, **5**, and **22** all displayed comparable, albeit less potent, activity to known antibacterials carbenicillin and kanamycin. Compounds **17** and **23**, which showed activity against Gram-positive *S. aureas*, were virtually inactive at 50 μM against Gram-negative *E. coli* (Fig. 5).

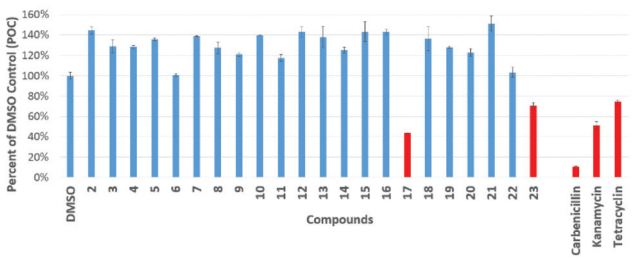

Fig. 3 Bacterial cell viability assay (*S. aureas*) using compounds **2**–**23** at 500 μM (BacTiter-Glo kit, Promega) and 8 h exposure. Values are shown as percent of DMSO control (POC). Values below 75% (stronger activity) are highlighted in red.

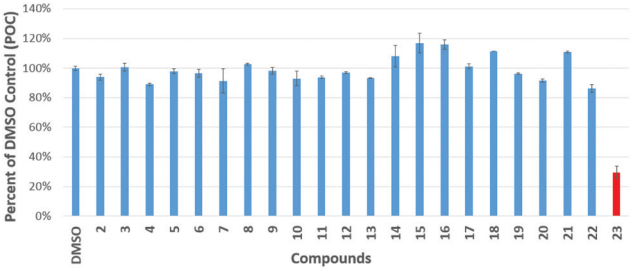

Fig. 4 Control experiment performed at 10 minutes exposure of 50 μM of compounds using luciferase-producing CellTiter-Glo assay with exogenous ATP added. Values are shown as percent of DMSO control (POC). Values below 50% (stronger activity) are highlighted in red.

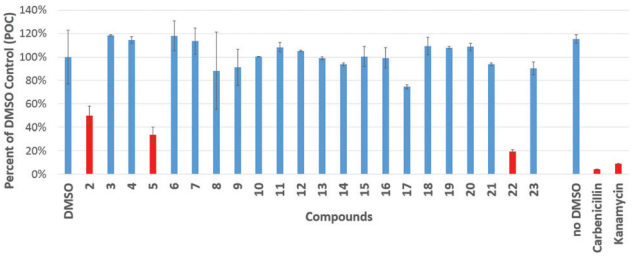

Fig. 5 Bacterial cell viability assay (*E. coli*) using compounds **2**–**23** at 50 μM (BacTiter-Glo kit, Promega) and 8 h exposure. Values are shown as percent of DMSO control (POC). Values below 50% (stronger activity) are highlighted in red.

With regard to structural variations of **2**–**23**, the presence of an electron-withdrawing substituent at the 4-position of the benzene portion of the sulfonamide such as a nitro group (compound **2**) or chloro (compounds **5** and **22**) appears to have some effect when comparing to analogous electron-donating substituents (for example, compound **22** *vs.* **23**). However, this structural feature is not solely responsible for activity, as evidenced by the inactivity of compounds **6** and **7**, which also contain an electron-withdrawing substitutent at the 4-position. In addition, the observed activity is not solely due to the presence of a nitro or chloro substituent on the aromatic ring of the sulfonamide. For example, when a nitro or chloro group is located at the 2- or 3-position (compounds **9**, **10**, and **12**) instead of the 4-position, loss of activity is observed. The presence of a substituent on the fluorene core also resulted in detrimental bactericidal effect as observed when comparing compound **5** with analogous compounds **20** and **21**. Although a predictable trend in structural features is unclear at this time, it is clearly evident that bactericidal effect is observed from sulfonamides generated from PAH scaffolds.

In vitro cytotoxicity screening of 2–23

In order to determine cytotoxicity towards mammalian cells, an initial cytotoxicity screening of library compounds (50 μM) using a variety of cell lines (diploid fibroblast – HDF; kidney – H293; cervical – HeLa; prostate – PC3; and pancreatic – BxPC3) was conducted using CellTiter-Blue Cell Viability (Promega) assay. The CellTiter-Blue assay is based upon the conversion of resazurin to the fluorescent resorufin by living cells, allowing for the quantification of living cells by fluorescence emission. The cells (~20 000 in 20 μL PBS) were treated with library compounds for 24 hours and the results are shown in Table 3 as percent of DMSO control (POC).

The results of the cell viability assays were verified by using an additional viability assay that has been reported to give comparable/similar results.[27] CellTiter-Glo operates similarly to BacTiter-Glo by measuring cell viability *via* quantification of ATP released from living cells by measurement of photoluminescent luciferase. The results obtained from cell viability screening using compounds **2–23** (50 μM) against the five cell lines using a CellTiter-Glo assay kit (ESI Table S1†) are in agreement with results from the CellTiter-Blue assay (Table 3).

Of the three compounds that displayed activity against *E. coli* at 50 μM (compounds **2**, **5**, and **22**), compounds **2** and **5** appear to be almost completely inactive against eukaryotic cells at 50 μM. However, compound **22** displays moderate activity against 4 of the 5 of the cell lines tested, with no activity observed against PC3 at 50 μM. With respect to the compounds that displayed bactericidal effect against Gram-positive *S. aureas* (compounds **17** and **23**), only compound **17** shows cytotoxicity towards the five cell lines at 50 μM. Regarding eukaryotic cytotoxicity of compounds **2–23**, moderate activity was observed from **14**, **15**, **21**, and **22**, and the strongest hit (defined herein as compounds with cell viability <50% POC) was compound **17** (Fig. 6).

Table 3 Cytotoxicity of compounds 2–23 at 50 μM

Percent of DMSO control (POC)[a] of various cell lines					
Cmpd	HDF	H293	HeLa	PC3	BxPC3
2	99.1 ± 1.5	96.8 ± 7.1	92.1 ± 4.8	100.9 ± 1.6	80.2 ± 9.3
3	80.8 ± 0.4	93.8 ± 7.0	87.7 ± 2.6	99.1 ± 0.5	75.8 ± 0.1
4	74.6 ± 2.7	93.0 ± 7.6	82.8 ± 0.3	81.8 ± 0.5	74.7 ± 2.9
5	81.0 ± 1.7	95.3 ± 5.5	81.8 ± 0.2	88.4 ± 2.8	81.3 ± 2.9
6	93.0 ± 5.2	69.6 ± 0.7	87.7 ± 2.1	103.3 ± 1.4	91.5 ± 2.2
7	76.9 ± 4.7	70.2 ± 2.0	81.0 ± 7.2	84.1 ± 0.1	72.1 ± 0.2
8	81.6 ± 4.6	94.7 ± 1.0	82.5 ± 1.7	91.7 ± 1.6	74.0 ± 5.7
9	104.5 ± 7.4	84.4 ± 0.5	89.0 ± 0.6	102.2 ± 5.0	93.6 ± 0.5
10	94.0 ± 2.0	67.4 ± 0.2	85.7 ± 3.4	100.2 ± 1.2	101.6 ± 0.5
11	97.0 ± 9.0	82.4 ± 3.2	82.2 ± 0.1	89.9 ± 2.2	77.0 ± 3.2
12	81.4 ± 0.8	102.4 ± 4.4	78.1 ± 0.2	79.5 ± 1.7	69.0 ± 4.5
13	81.0 ± 9.0	100.5 ± 8.9	72.4 ± 0.1	75.0 ± 0.9	70.0 ± 1.7
14	**41.2 ± 0.8**	67.4 ± 0.5	**37.4 ± 1.0**	66.3 ± 6.1	**34.3 ± 5.7**
15	**49.3 ± 4.5**	71.3 ± 11.9	54.7 ± 4.4	66.7 ± 1.4	56.6 ± 4.3
16	69.5 ± 2.0	59.4 ± 2.7	75.9 ± 1.9	81.8 ± 4.2	60.6 ± 0.5
17	**30.7 ± 5.3**	**19.0 ± 2.9**	**34.1 ± 0.5**	**36.4 ± 0.8**	**12.8 ± 0.6**
18	74.4 ± 2.6	68.5 ± 0.0	68.5 ± 5.9	93.6 ± 2.5	73.7 ± 2.7
19	99.0 ± 8.0	99.5 ± 8.4	88.5 ± 0.9	84.2 ± 1.3	84.9 ± 5.5
20	87.5 ± 8.2	82.4 ± 0.5	86.1 ± 3.4	100.4 ± 1.6	83.6 ± 5.1
21	55.9 ± 4.4	**38.1 ± 4.4**	69.2 ± 10.6	99.3 ± 1.7	**46.9 ± 3.5**
22	**34.2 ± 3.8**	61.7 ± 7.1	**46.5 ± 3.7**	99.2 ± 1.9	65.3 ± 2.0
23	106.0 ± 4.8	83.5 ± 13.6	78.4 ± 0.2	91.1 ± 2.3	98.2 ± 4.0

[a] All values (%) against 5 cell lines were obtained as an average of duplicate measurements *via* the CellTiter-Blue (Promega) assay at 50 μM (24 h). Lower values of POC indicate stronger hits. POC values below 50% are highlighted in bold.

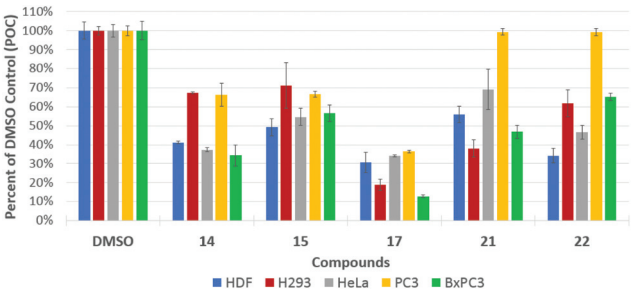

Fig. 6 Cell viability screening of compounds **14**, **15**, **17**, **21** and **22** from Table 3 performed at 50 μM with HDF, H293, HeLa, PC3, and BxPC3 cell lines. Values are shown as POC (percent of control).

Experimental and *in silico* predictions for drug-likeness and physicochemical properties of 2–23

Several approaches have recently been developed for the prediction of drug-likeness of bioactive compounds based upon certain properties such as molecular weight, water solubility, lipophilicity, topological factors, and adherence to general drug-likeness parameters. Using two open-source programs, OSIRIS Property Explorer[28] and SwissADME,[29] the *in silico* assessment of the properties and drug-likeness of compounds **2–23** was explored and is summarized in Table 4 and in Table S2 in the ESI.†

With regard to molecular weight, it is estimated that the majority of drugs have a molecular weight ranging from 200 to 450 g mol^{-1}. All library compounds, with the exception of the iodine-containing **21**, fall into this acceptable range. Topological polar surface area (TPSA) is a metric commonly used to predict a drug's ability to permeate cells. Molecules with a TPSA below 140 angstroms are considered within range for cell permeation, and compounds **2–23** all have values lower than 140 (Table 4). TPSA values lower than 90 are also used to predict the capability of a molecule to cross the blood–brain barrier. The fluorene scaffold imparts a significant lipophilicity to the overall molecule in each example, and this is evidenced by the *c*log *P* values experimentally determined for **2–23**. The log *P* value of a compound is the logarithm of its partition coefficient between *n*-octanol and water [$\log(c_{\text{octanol}})/(c_{\text{water}})$]. It has been established that most drugs have *c*log *P* values less than 5.0, and compounds **2–23**, with the exceptions of **18** and **21**, are all determined to be within acceptable range. The *c*log *P* values predicted using SwissADME software closely matched the values experimentally obtained (Table S2, ESI†). In addition, the vast majority of drugs on the market have log *S* (water solubility) values that range between 0.0 and −6.0. The majority of compounds **2–23** fall within this range, includ-

Table 4 Drug-likeness and physicochemical properties of compounds **2–23** as experimentally determined or predicted by OSIRIS and SwissADME

Cmpd	MW	TPSA[a]	*c* log *P*[b]	log *S*[c]	log K_p[d]	Drug score[e]
2	368	100.4	3.69	−4.04	−6.06	0.38
3	335	54.6	3.96	−5.10	−5.40	0.10
4	351	63.8	3.57	−4.77	−5.78	0.11
5	356	54.6	4.30	−5.49	−5.34	0.09
6	389	54.6	4.48	−5.53	−5.36	0.08
7	339	54.6	3.70	−5.07	−5.62	0.11
8	321	54.6	3.49	−4.75	−5.58	0.11
9	366	100.4	3.59	−5.21	−5.97	0.11
10	356	54.6	4.29	−5.49	−5.34	0.09
11	339	54.6	3.77	−5.07	−5.62	0.11
12	356	54.6	3.67	−5.49	−5.34	0.09
13	339	54.6	3.38	−5.07	−5.62	0.11
14	357	54.6	3.67	−5.38	−5.65	0.10
15	357	54.6	3.13	−5.38	−5.65	0.10
16	357	54.6	4.16	−5.38	−5.65	0.10
17	411	54.6	4.43	−6.32	−5.77	0.08
18	425	54.6	5.17	−6.96	−4.87	0.04
19	259	54.6	1.80	−4.51	−6.31	0.14
20	435	54.6	4.99	−6.32	−5.33	0.11
21	482	54.6	5.08	−6.50	−5.65	0.12
22	388	79.9	2.15	−5.19	−5.22	0.46
23	383	89.1	0.86	−4.47	−5.66	0.57

[a] TPSA = Topological polar surface area; calculated by SwissADME. [b] Experimentally obtained. [c] Solubility (log *S*) calculated by OSIRIS. [d] Indicates skin permeation in cm s^{-1}; calculated by SwissADME. [e] Calculated by OSIRIS.

ing the bactericidal compounds **2**, **5**, **22**, and **23**. Additional graphical summaries and BOILED-Egg plots[30] of **2–23** generated by SwissADME are found within the ESI.†

In terms of drug-likeness, 5 different sets (Lipinski, Ghose, Veber, Egan, and Muegge) of rules and/or parameters used within medicinal chemistry to predict the likelihood of a molecule to be a drug candidate were applied using SwissADME (Table S2, ESI†).[29] The bactericidal compounds **2**, **5**, and **23** display no violations of any of the drug-likeness parameters. Lastly, the drug score calculated by OSIRIS combines drug-likeness, *c*log *P*, log *S*, MW, and toxicity risks into one composite value in order to predict a compound's overall potential as a drug.[28] Interestingly, the three highest drug scores calculated from compounds **2–23** belong to the bactericidal compounds, **2**, **22**, and **23**.

Conclusions

In conclusion, a new method for direct substitution of a 2° C(sp^3)–X bond with a sulfonamide unit using a $PhI(OAc)_2/I_2$ system is reported. The method is speculated to operate *via* a mechanism involving a NCR species according to experimental observations. Key aspects of the approach include mild reaction temperature, non-metal activation, and the use of readily available and stable reagents. Using the new method, a series of 9-aminosulfonyl fluorene analogs as well as heteroanthracene products were generated. Biological activity of the synthesized compounds was evaluated using a BacTiter-Glo cell viability assay with Gram-positive (*Staphylococcus aureas*) and Gram-negative (*E. coli*) bacterial strains. Compounds **17** and **23** are active (comparable to positive controls) at 500 μM against *S. aureas* and compounds **2**, **5**, and **22** are active at 50 μM against *E. coli* (comparable to positive controls). In addition to screening for bactericidal activity, the effect of the compounds on a series of mammalian cell lines (HDF, H293, HeLa, PC3, and BxPC3) was determined using CellTiter-Blue and CellTiter-Glo cell viability assays. Bactericidal compounds **2**, **5**, **22**, and **23** have significantly lower, or negligible, activity against mammalian cell lines at 50 μM concentration. In addition, compound **23** was discovered as a luciferase inhibitor. Finally, the experimental determination of compound **2–23** lipophilicity values (*c* log *P*) along with *in silico*-generated physicochemical properties and predictions are provided. Although product yields in some examples are relatively modest, we believe this work will serve to support the consideration of fluorene-scaffold compounds as potential antibacterial drugs that warrant further synthetic exploration.

Experimental

Materials and instrumentation (synthesis)

All reagents and solvents were purchased from commercial sources and used without further purification. I_2 was purchased from Alfa Aesar in 99.99+% purity (metals basis). ^1H and ^{13}C NMR spectra were recorded on a Varian 400/100 (400 MHz) spectrometer in deuterated chloroform ($CDCl_3$) or deuterated acetone ($(CD_3)_2CO$) with the solvent residual peak as internal reference unless otherwise stated ($CDCl_3$: ^1H = 7.26 ppm, ^{13}C = 77.02 ppm; $(CD_3)_2CO$: ^1H = 2.05 ppm, ^{13}C = 29.84 ppm). Data are reported in the following order: Chemical shifts (δ) are reported in ppm, and spin–spin coupling constants (J) are reported in Hz, while multiplicities are abbreviated by s (singlet), bs (broad singlet), d (doublet), dd (doublet of doublets), t (triplet), dt (double of triplets), td (triplet of doublets), m (multiplet). Infrared spectra were recorded on a Nicolet iS50 FT-IR spectrometer, and peaks are reported in reciprocal centimeters (cm^{-1}). Melting points were recorded on a Mel-Temp II (Laboratory Devices, USA) and were uncorrected. MS (EI) were obtained using a Shimadzu GC-2010 Plus with GCMS-QP2010. Accurate mass spectrum (HRMS-High Resolution Mass Spectrometry) was performed using a Thermo Scientific Exactive spectrometer (Waltham, MA, USA) operating in positive and negative mode (ESI-electrospray ionization).

General procedure for the synthesis of *N*-alkyl sulfonamides

To an oven-dried reaction tube was added polycyclic hydrocarbon substrate (0.5 mmol, 2 equiv.), sulfonamide (0.25 mmol, 1 equiv.), iodobenzene diacetate (0.5 mmol, 2 equiv.), I_2 (0.25 mmol, 1 equiv.) in dry DCM (3–4 mL). The mixture was stirred at 50 °C under argon for 24 hours. After 24 hours, the reaction was cooled to room temperature and the solvent was removed under vacuum. Crude sulfonamide

was purified by flash chromatography using hexanes : EtOAc. In some cases, a minimal amount of DCM was used to help solubilize the solid prior to chromatography.

Procedure for gram scale synthesis of product 5

To an oven-dried reaction flask was added 9-bromofluorene (2.45 g, 10.0 mmol), 4-chlorobenzenesulfonamide (0.958 g, 5.0 mmol), iodobenzene diacetate (3.22 g, 10.0 mmol), I_2 (1.27 g, 5.0 mmol) in dry DCM (50 mL). The mixture was stirred at 50 °C under argon for 24 hours. After 24 hours, the reaction was cooled to room temperature and the solvent was removed under vacuum. Crude sulfonamide was purified by flash chromatography using 4 : 1 hexanes/EtOAc resulting in isolation of 1.207 g (68%) of product **5**.

Materials and methods (Bioactivity assays)

E. coli (JM109) and *S. aureas* (MicroKwik) were each (separately) grown overnight in Circle Grow broth plus 50 μg mL^{-1} Amp. The overnight culture (10 μL) was diluted into 21 mL of fresh Circle Grow plus Amp. Aliquots were withdrawn (approximately 10 000 cells), treated with DMSO or 50 μM library compounds, then placed in a 96-well plate at 37 °C with shaking to initiate cell growth for 8 hours. After 8 hours, cell viability was determined by adding 10 μL BacTiter-Glo reagent (Ultra-Glo Recombinant Luciferase) for 5–10 minutes (following protocol issued by Promega). Luminescence was measured using a Promega Glomax Multi + detection system.

Cell-based Glo kits, such as CellTiter-Blue and CellTiter-Glo were obtained from Promega (Madison, WI, USA). All cell cultures were obtained from the American Type Culture Collection (ATCC, Manassas, VA, USA). All other materials and supplies were purchased from commercial sources and used without additional purification. Cell cultures were maintained in DMEM (Fisher Scientific) supplemented with 10% fetal bovine serum and Penn/Strep. Cultures were maintained in a 37 °C water-jacketed incubator with 5% CO_2. For experiments in 96-well plates, proliferating cells were removed from the stock plate using PBS plus 2.5 mM EDTA. The desired number of cells (~20 000) were distributed in a 96-well plate containing 100 μL DMEM plus 10% FBS and allowed to attach overnight. After 24 hours, cells were treated with the indicated library compound **2–23** or DMSO control (5%). After a set time (24 hours for CellTiter-Blue and 2 hours for CellTiter-Glo), cell viability was determined by adding 10 μL CellTiter-Blue or CellTiter-Glo reagent for 1–4 hours. Fluorescence was measured either on a TECAN Safire plate reader (ex^{560}/em^{590}) or using a Promega Glomax Multi + detection system.

Experimental *c* log *P* Determination

The method of log *P* determination followed literature precedent.[31] Samples were prepared by dissolving approximately 1 mg of library compound in 1 mL of ethyl acetate. Samples were analyzed by HPLC (Agilent 1100 Series, 210 nm) using an isocratic, 75% methanol/25% water mobile phase at a rate of 1 mL min^{-1} over a 25 cm Discovery C18 stationary phase. The capacity factors (k') of the compounds were calculated using the formula $[k' = (t_R - t_m)/t_m]$ where t_R is the retention time of the sample compound and t_m is the retention time of the solvent (ethyl acetate). To create a reference calibration curve, the log of the capacity factors was plotted against the reported partition coefficient (log *P*) values for 6 reference compounds (Fig. S3, ESI†). Using the reference calibration curve, linear regression coefficients "*a*" and "*b*" were determined. For library compounds **2–23**, the partition coefficient (log *P*) was determined by using the experimentally determined capacity factor (k') and the linear regression coefficients obtained from the calibration curve in the formula $[\log P = a + b\ (\log k')]$.

Compound characterization

***N*-(9*H*-Fluoren-9-yl)-4-nitrobenzenesulfonamide (2).** White solid (44 mg, 48%). M.p. 228–230 °C. Purification (hexanes : EtOAc, 80 : 20). R_f = 0.32. ^{1}H NMR (400 MHz, $CDCl_3$): δ = 8.46 (dt, J_1 = 9.0 Hz, J_2 = 2.0 Hz, 2H), 8.24 (dt, J_1 = 9.0 Hz, J_2 = 2.0 Hz, 2H), 7.65 (d, J_1 = 7.4 Hz, 2H), 7.39 (m, 2H), 7.24 (m, 4H), 5.47 (d, J_1 = 9.4 Hz, 1H), 4.95 (d, J_1 = 9.4 Hz, 1H) ppm. ^{13}C NMR (100 MHz, $CDCl_3$): δ 147.3, 142.5, 140.1, 129.4, 128.4, 128.1, 125.0, 124.7, 124.6, 120.2, 58.7 ppm. IR (neat): ν = 3283, 3109, 1519, 1334, 1313, 1157, 1059, 854, 737, 611 cm^{-1}. HRMS (ESI): calculated for $C_{19}H_{13}N_2O_4S$ $[M - H]^+$ requires *m*/*z* 365.05961, found *m*/*z* 365.05890.

***N*-(9*H*-Fluoren-9-yl)-4-methylbenzenesulfonamide (3).**[20b] White solid (70 mg, 83%). M.p. 198–200 °C. Purification (hexanes : EtOAc, 80 : 20). R_f = 0.37. ^{1}H NMR (400 MHz, $CDCl_3$): δ = 7.94 (dt, J_1 = 8.6 Hz, J_2 = 2.0 Hz, 2H), 7.60 (d, J_1 = 7.4 Hz, 2H), 7.41 (d, J_1 = 8.2 Hz, 2H), 7.34 (m, 2H), 7.20 (m, 4H), 5.38 (d, J_1 = 9.4 Hz, 1H), 4.78 (d, J_1 = 9.4 Hz, 1H), 2.51 (s, 3H) ppm. ^{13}C NMR (100 MHz, $CDCl_3$): δ 143.8, 143.3, 140.0, 138.4, 130.0, 129.0, 127.8, 127.3, 125.2, 119.9, 58.3, 21.6 ppm. IR (neat): ν = 3304, 3032, 2919, 1597, 1448, 1324, 1153, 1093, 756, 543 cm^{-1}. HRMS (ESI): calculated for $C_{20}H_{17}NO_2SNa$ $[M + Na]^+$ requires *m*/*z* 358.08777, found *m*/*z* 358.09146.

***N*-(9*H*-Fluoren-9-yl)-4-methoxybenzenesulfonamide (4).** White solid (60 mg, 68%). M.p. 178–181 °C. Purification (hexanes : EtOAc, 80 : 20). R_f = 0.21. ^{1}H NMR (400 MHz, $CDCl_3$): δ = 8.01 (dd, J_1 = 7.0 Hz, J_2 = 2.3 Hz, 2H), 7.63 (d, J_1 = 7.4 Hz, 2H), 7.36 (m, 2H), 7.25 (m, 4H), 7.08 (dd, J_1 = 7.0 Hz, J_2 = 2.3 Hz, 2H), 5.39 (d, J_1 = 9.4 Hz, 1H), 4.75 (d, J_1 = 9.4 Hz, 1H), 3.93 (s, 3H) ppm. ^{13}C NMR (100 MHz, $CDCl_3$): δ 163.1, 143.4, 140.0, 132.9, 129.5, 129.0, 127.9, 125.2, 120.0, 114.5, 58.4, 55.7 ppm. IR (neat): ν = 3282, 2928, 2842, 1594, 1327, 1180, 1094, 743, 570 cm^{-1}. HRMS (ESI): calculated for $C_{20}H_{17}NO_3SNa$ $[M + Na]^+$ requires *m*/*z* 374.08269, found *m*/*z* 374.08749.

4-Chloro-*N*-(9*H*-fluoren-9-yl)benzenesulfonamide (5).[20b] White solid (63 mg, 70%). M.p. 202–205 °C. Purification (hexanes : EtOAc, 80 : 20). R_f = 0.43. ^{1}H NMR (400 MHz, $CDCl_3$): δ = 7.99 (dt, J_1 = 9.0 Hz, J_2 = 2.4 Hz, 2H), 7.60 (m, 4H), 7.36 (ddd, J_1 = 7.8 Hz, J_2 = 4.7 Hz, J_3 = 3.5 Hz, 2H), 7.23 (m, 4H), 5.40 (d, J_1 = 9.4 Hz, 1H), 4.85 (d, J_1 = 9.4 Hz, 1H) ppm. ^{13}C NMR (100 MHz, $CDCl_3$): δ 142.9, 140.0, 132.2, 129.8, 129.7, 129.2, 128.7, 128.0, 125.1, 120.1, 58.5 ppm. IR (neat): ν = 3272, 3090, 2925, 1399, 1328, 1164, 1084, 745 cm^{-1}. HRMS (ESI): cal-

culated for $C_{19}H_{13}ClNO_2S$ $[M - H]^+$ requires *m*/*z* 354.03555, found *m*/*z* 354.03586.

***N*-(9*H*-Fluoren-9-yl)-4-(trifluoromethyl)benzenesulfonamide (6).** White solid (57 mg, 58%). M.p. 206–209 °C. Purification (hexanes : EtOAc, 80 : 20). R_f = 0.44. ^{1}H NMR (400 MHz, $CDCl_3$): δ = 8.18 (d, J_1 = 7.8 Hz, 2H), 7.89 (d, J_1 = 7.8 Hz, 2H), 7.63 (d, J_1 = 7.4 Hz, 2H), 7.37 (td, J_1 = 7.3 × (2) Hz, J_2 = 1.4 Hz, 2H), 7.21 (m, 4H), 5.44 (d, J_1 = 9.8 Hz, 1H), 4.89 (d, J_1 = 9.4 Hz, 1H) ppm. ^{13}C NMR (100 MHz, $CDCl_3$): δ 145.1, 142.7, 140.1, 132.3, 129.3, 128.0, 127.7, 126.6 (q, J_1 = 3.7 × (3) Hz), 125.0, 120.1, 58.6 ppm. IR (neat): ν = 3296, 3059, 1404, 1327, 1123, 1062, 711, 607 cm^{-1}. HRMS (ESI): calculated for $C_{20}H_{13}F_3NO_2S$ $[M - H]^+$ requires *m*/*z* 388.06191, found *m*/*z* 388.06161.

***N*-(9*H*-Fluoren-9-yl)-4-fluorobenzenesulfonamide (7).** White solid (42 mg, 50%). M.p. 209–212 °C (hexanes : EtOAc 80 : 20). R_f = 0.40. ^{1}H NMR (400 MHz, $(CD_3)_2CO$): δ = 8.19 (m, 2H), 7.75 (d, J_1 = 7.4 Hz, 2H), 7.49 (m, 2H), 7.38 (t, J_1 = 6.7 × (2) Hz, 2H), 7.25 (td, J_1 = 7.4 × (2) Hz, J_2 = 1.2 Hz, 3H), 7.19 (d, J_1 = 7.4 Hz, 2H), 5.45 (d, J_1 = 8.6 Hz, 1H) ppm. ^{13}C NMR (100 MHz, $(CD_3)_2CO$): δ 165.8 (d, J_1 = 252.8 Hz), 144.7, 140.9, 130.9, 130.8, 129.6, 128.5, 125.9, 120.8, 117.4, 117.2, 59.2 ppm. IR (neat): ν = 3268, 3065, 1590, 1495, 1329, 1169, 1161, 1092, 848, 738, 560 cm^{-1}. HRMS (ESI): calculated for $C_{19}H_{13}FNO_2S$ $[M - H]^+$ requires *m*/*z* 338.06510, found *m*/*z* 338.06516.

***N*-(9*H*-Fluoren-9-yl)benzenesulfonamide (8).**[20b] White solid (36 mg, 44%). M.p. 214–218 °C. Purification (hexanes : EtOAc, 80 : 20). R_f = 0.32. ^{1}H NMR (400 MHz, $CDCl_3$): δ = 8.07 (dt, J_1 = 8.6 Hz, J_2 = 2.7 Hz, 2H), 7.70 (m, 1H), 7.63 (m, 4H), 7.35 (td, J_1 = 7.2 × (2) Hz, J_2 = 1.2 Hz, 2H), 7.20 (m, 4H), 5.42 (d, J_1 = 9.4 Hz, 1H), 4.79 (d, J_1 = 9.4 Hz, 1H) ppm. ^{13}C NMR (100 MHz, $CDCl_3$): δ 143.2, 141.4, 140.0, 133.0, 129.4, 129.0, 127.9, 127.3, 125.2, 120.0, 58.5 ppm. IR (neat): ν = 3252, 3067, 1447, 1327, 1163, 1153, 739, 618, 559 cm^{-1}. HRMS (ESI): calculated for $C_{19}H_{15}NO_2SNa$ $[M + Na]^+$ requires *m*/*z* 344.07212, found *m*/*z* 344.07611.

***N*-(9*H*-Fluoren-9-yl)-3-nitrobenzenesulfonamide (9).** White solid (23 mg, 25%). M.p. 208–210 °C. Purification (hexanes : EtOAc, 80 : 20). R_f = 0.19. ^{1}H NMR (400 MHz, $CDCl_3$): δ = 8.89 (t, J_1 = 2.0 × (2) Hz, 1H), 8.53 (ddd, J_1 = 8.2 Hz, J_2 = 2.0 Hz, J_3 = 1.0 Hz, 1H), 8.37 (dt, J_1 = 7.8 Hz, J_2 = 1.0 × (2) Hz, 1H), 7.84 (t, J_1 = 8.0 × (2) Hz, 1H), 7.65 (dd, J_1 = 7.4 Hz, J_2 = 1.0 Hz, 2H), 7.38 (m, 2H), 7.24 (m, 4H), 5.47 (d, J_1 = 9.0 Hz, 1H), 4.99 (d, J_1 = 9.0 Hz, 1H) ppm. ^{13}C NMR (100 MHz, $CDCl_3$): δ 148.4, 143.7, 142.4, 140.1, 132.6, 130.8, 129.4, 128.0, 127.4, 125.0, 122.5, 120.2, 58.7 ppm. IR (neat): ν = 3327, 3082, 2926, 1531, 1355, 1169, 589 cm^{-1}. HRMS (ESI): calculated for $C_{19}H_{13}N_2O_4S$ $[M - H]^+$ requires *m*/*z* 365.05961, found *m*/*z* 365.05981.

3-Chloro-*N*-(9*H*-fluoren-9-yl)benzenesulfonamide (10). Off-white solid (46 mg, 52%). M.p. 165–168 °C. Purification (hexanes : EtOAc 80 : 20). R_f = 0.43. ^{1}H NMR (400 MHz, $CDCl_3$): δ = 8.05 (t, J_1 = 1.8 × (2) Hz, 1H), 7.93 (dt, J_1 = 7.8 Hz, 1H), 7.66 (ddd, J_1 = 9.8 Hz, J_2 = 7.8 Hz, J_3 = 0.8 Hz, 1H), 7.61 (d, J_1 = 7.4 Hz, 2H), 7.57 (t, J_1 = 7.8 × (2) Hz, 1H), 7.36 (m, 2H), 7.23 (m, 4H), 5.40 (d, J_1 = 9.4 Hz, 1H), 4.90 (d, J_1 = 9.4 Hz, 1H) ppm. ^{13}C NMR (100 MHz, $CDCl_3$): δ 143.1, 142.8, 140.0, 135.5, 133.0, 130.7, 129.2, 127.9, 127.3, 125.2, 125.1, 120.0, 58.5 ppm. IR (neat): ν = 3279, 3067, 2922, 1427, 1337, 1159, 1050, 742 cm^{-1}. HRMS (ESI): calculated for $C_{19}H_{13}ClNO_2S$ $[M - H]^+$ requires *m*/*z* 354.03555, found *m*/*z* 354.03619.

***N*-(9*H*-Fluoren-9-yl)-3-fluorobenzenesulfonamide (11).** Off-white solid (27 mg, 32%). M.p. 152–155 °C. Purification (hexanes : EtOAc 80 : 20). R_f = 0.39. ^{1}H NMR (400 MHz, $CDCl_3$): δ = 7.86 (d, J_1 = 7.0 Hz, 1H), 7.77 (dt, J_1 = 8.0 Hz, J_2 = 2.2 × (2) Hz, 1H), 7.62 (m, 2H), 7.38 (m, 4H), 7.22 (m, 4H), 5.42 (d, J_1 = 9.4 Hz, 1H), 4.87 (d, J_1 = 9.4 Hz, 1H) ppm. ^{13}C NMR (100 MHz, $CDCl_3$): δ 162.6 (d, J_1 = 250.8 Hz), 143.5 (d, J_1 = 7.0 Hz), 142.9, 140.0, 131.3 (d, J_1 = 7.7 Hz), 129.2, 128.0, 125.1, 123.0 (d, J_1 = 3.3 Hz), 120.2 (d, J_1 = 21.4 Hz), 120.1, 114.7 (d, J_1 = 24.3 Hz), 58.5 ppm. IR (neat): ν = 3277, 2927, 2874, 1708, 1447, 1151, 1058, 733 cm^{-1}. HRMS (ESI): calculated for $C_{19}H_{13}FNO_2S$ $[M - H]^+$ requires *m*/*z* 338.06510, found *m*/*z* 338.06534.

2-Chloro-*N*-(9*H*-fluoren-9-yl)benzenesulfonamide (12). White solid (54 mg, 60%). M.p. 106–108 °C. Purification (hexanes : EtOAc, 80 : 20). R_f = 0.34. ^{1}H NMR (400 MHz, $CDCl_3$): δ = 8.29 (dd, J_1 = 7.6 Hz, J_2 = 1.4 Hz, 1H), 7.64 (m, 4H), 7.51 (m, 1H), 7.37 (td, J_1 = 7.0 Hz, J_2 = 1.4 Hz, 2H), 7.29 (m, 2H), 7.23 (td, J_1 = 7.4 Hz, J_2 = 1.4 Hz, 2H), 5.44 (d, J_1 = 9.0 Hz, 1H), 5.32 (d, J_1 = 9.0 Hz, 1H) ppm. ^{13}C NMR (100 MHz, $CDCl_3$): δ 142.9, 140.1, 138.8, 133.9, 131.82, 131.8, 131.0, 129.1, 127.9, 127.4, 125.2, 120.0, 58.8 ppm. IR (neat): ν = 3348, 3293, 3066, 1707, 1451, 1337, 1160, 1043, 742, 585, 558 cm^{-1}. HRMS (ESI): calculated for $C_{19}H_{13}ClNO_2S$ $[M - H]^+$ requires *m*/*z* 354.03555, found *m*/*z* 354.03610.

***N*-(9*H*-Fluoren-9-yl)-2-fluorobenzenesulfonamide (13).** Off-white solid (37 mg, 44%). M.p. 208–210 °C (hexanes : EtOAc 80 : 20). R_f = 0.36. ^{1}H NMR (400 MHz, $CDCl_3$): δ = 8.09 (td, J_1 = 7.5 × (2) Hz, J_2 = 1.8 Hz, 1H), 7.69 (m, 1H), 7.65 (d, J_1 = 7.4 Hz, 2H), 7.38 (m, 4H), 7.33 (d, J_1 = 7.4 Hz, 2H), 7.24 (dd, J_1 = 7.4 Hz, J_2 = 0.8 Hz, 2H), 5.52 (d, J_1 = 9.4 Hz, 1H), 5.08 (d, J_1 = 9.4 Hz, 1H) ppm. ^{13}C NMR (100 MHz, $CDCl_3$): δ 158.9 (d, J_1 = 255.1 Hz), 143.0, 140.1, 135.2 (d, J_1 = 8.2 Hz), 130.1, 129.1, 127.9, 125.2, 124.7, 117.2 (d, J_1 = 20.9 Hz), 58.7 ppm. IR (neat): ν = 3264, 2920, 2850, 1474, 1334, 1168, 1076, 737 cm^{-1}. HRMS (ESI): calculated for $C_{19}H_{13}FNO_2S$ $[M - H]^+$ requires *m*/*z* 338.06510, found *m*/*z* 338.06570.

***N*-(9*H*-Fluoren-9-yl)-2,4-difluorobenzenesulfonamide (14).** White solid (40 mg, 45%). M.p. 146–149 °C. Purification (hexanes : EtOAc, 90 : 10). R_f = 0.19. ^{1}H NMR (400 MHz, $CDCl_3$): δ = 8.07 (q, J_1 = 7.0 × (3) Hz, 1H), 7.62 (d, J_1 = 7.4 Hz, 2H), 7.35 (m, 4H), 7.25 (m, 2H), 7.06 (m, 2H), 5.47 (d, J_1 = 9.0 Hz, 1H), 5.06 (d, J_1 = 9.0 Hz, 1H) ppm. ^{13}C NMR (100 MHz, $CDCl_3$) δ 167.2 (dd, J_1 = 257.3 Hz, J_2 = 11.2 Hz), 159.7 (dd, J_1 = 257.3 Hz, J_2 = 12.7 Hz), 142.8, 140.1, 131.8 (d, J_1 = 10.5 Hz), 129.2, 128.0, 125.1, 120.1, 112.0 (dd, J_1 = 20.9 Hz, J_2 = 3.0 Hz), 105.8 (t, J_1 = 26.2 × (2) Hz), 58.7 ppm. IR (neat): ν = 3271, 2921, 2849, 1602, 1340, 1167, 1148, 1075, 970, 851, 757 cm^{-1}. HRMS (ESI): calculated for $C_{19}H_{13}F_2NO_2SNa$ $[M + Na]^+$ requires *m*/*z* or 380.05328, found *m*/*z* 380.05356.

***N*-(9*H*-Fluoren-9-yl)-2,6-difluorobenzenesulfonamide (15).** White solid (66 mg, 74%). M.p. 166–170 °C. Purification (hexanes : EtOAc, 80 : 20). R_f = 0.27. ^{1}H NMR (400 MHz, $CDCl_3$): δ = 7.61 (m, 3H), 7.36 (m, 4H), 7.24 (t, J_1 = 7.4 × (2) Hz, 2H),

7.13 (t, J_1 = 8.6 Hz, 2H), 5.60 (d, J_1 = 9.0 Hz, 1H), 5.27 (d, J_1 = 9.0 Hz, 1H) ppm. ^{13}C NMR (100 MHz, $CDCl_3$): δ 159.5 (dd, J_1 = 257.3 Hz, J_2 = 3.8 Hz), 142.7, 140.1, 134.5 (t, J_1 = 11.0 Hz), 129.2, 127.9, 125.1, 120.1, 119.8 (m), 113.3 (dd, J_1 = 23.2 Hz, J_2 = 3.7 Hz), 58.8 ppm. IR (neat): ν = 3274, 3041, 1610, 1466, 1352, 1269, 1168, 1003, 735 cm^{-1}. HRMS (ESI): calculated for $C_{19}H_{13}F_2NO_2SNa$ $[M + Na]^+$ requires *m*/*z* or 380.05328, found *m*/*z* 380.05588.

***N*-(9*H*-Fluoren-9-yl)-3,5-difluorobenzenesulfonamide (16).** White solid (49 mg, 54%). M.p. 190–192 °C (hexanes : EtOAc 90 : 10). R_f = 0.23. ^{1}H NMR (400 MHz, $CDCl_3$): δ = 7.58 (d, J_1 = 7.4 Hz, 2H), 7.53 (d, J_1 = 3.9 Hz, 2H), 7.34 (td, J_1 = 7.4 × (2) Hz, J_2 = 1.2 Hz, 2H), 7.22 (m, 4H), 7.12 (tt, J_1 = 8.2 × (2) Hz, J_2 = 2.3 × (2) Hz, 1H), 5.36 (d, J_1 = 9.8 Hz, 1H), 4.89 (d, J_1 = 9.8 Hz, 1H) ppm. ^{13}C NMR (100 MHz, $CDCl_3$): δ 163.0 (dd, J_1 = 253.8, J_2 = 11.5 Hz), 144.8 (t, J_1 = 8.3 Hz), 142.6, 140.0, 129.3, 128.0, 125.0, 120.1, 110.7 (m), 108.5 (t, J_1 = 24.9 Hz), 58.6 ppm. IR (neat): ν = 3288, 3084, 1605, 1436, 1337, 1297, 1159, 1061, 1003, 743, 611 cm^{-1}. HRMS (ESI): calculated for $C_{19}H_{14}F_2NO_2S$ $[M + H]^+$ requires *m*/*z* 380.05328, found *m*/*z* 380.05643.

***N*-(9*H*-Fluoren-9-yl)-2,3,4,5,6-pentafluorobenzenesulfonamide (17).** White solid (59 mg, 58%). M.p. 144–148 °C. Purification (hexanes : EtOAc, 90 : 10 followed by 100% DCM). R_f = 0.74. ^{1}H NMR (400 MHz, $CDCl_3$): δ = 7.61 (d, J_1 = 7.8 Hz, 2H), 7.37 (m, 4H), 7.26 (t, J_1 = 7.4 × (2) Hz, 2H), 5.58 (d, J_1 = 9.0 Hz, 1H), 5.36 (d, J_1 = 9.0 Hz, 1H) ppm. ^{13}C NMR (100 MHz, $CDCl_3$): δ 145.7 (m), 143.2 (m), 142.0, 140.2, 136.7 (m), 129.5, 128.0, 125.0, 120.2, 117.8 (m), 59.0 ppm. IR (neat): ν = 3312, 2923, 1641, 1494, 1362, 1170, 1096, 9991, 740 cm^{-1}. HRMS (ESI): calculated for $C_{19}H_{10}F_5NO_2SNa$ $[M + Na]^+$ requires *m*/*z* or 434.02501, found *m*/*z* 434.02670.

2,4,6-Trichloro-*N*-(9*H*-fluoren-9-yl)benzenesulfonamide (18). White solid (51 mg, 48%). M.p. 212–214 °C (hexanes : EtOAc 90 : 10). R_f = 0.38. ^{1}H NMR (400 MHz, $CDCl_3$): δ = 7.65 (d, J_1 = 7.4 Hz, 2H), 7.58 (s, 2H), 7.39 (t, J_1 = 7.2 × (2) Hz, 2H), 7.28 (m, 4H), 5.60 (d, J_1 = 9.0 Hz, 1H), 5.56 (d, J_1 = 9.0 Hz, 1H) ppm. ^{13}C NMR (100 MHz, $CDCl_3$): δ 142.6, 140.2, 138.2, 135.8, 135.7, 131.3, 129.3, 128.0, 125.1, 120.1, 58.9 ppm. IR (neat): ν = 3275, 3057, 1560, 1364, 1171, 738 cm^{-1}. HRMS (ESI): calculated for $C_{19}H_{11}Cl_3NO_2S$ $[M - H]^-$ requires *m*/*z* 421.95761, found *m*/*z* 421.95398.

***N*-(9*H*-Fluoren-9-yl)methanesulfonamide (19).** White solid (27 mg, 40%). M.p. 180–182 °C. Purification (hexanes : EtOAc, 80 : 20). R_f = 0.13. ^{1}H NMR (400 MHz, $CDCl_3$): δ = 7.66 (dd, J_1 = 7.4 Hz, J_2 = 1.2 Hz, 4H), 7.40 (td, J_1 = 7.4 × (2) Hz, 2H), 7.33 (td, J_1 = 7.4 Hz, 2H), 5.50 (d, J_1 = 9.8 Hz, 1H), 4.60 (d, J_1 = 9.8 Hz, 1H), 3.24 (s, 3H) ppm. ^{13}C NMR (100 MHz, $CDCl_3$): δ 143.3, 140.1, 129.2, 128.0, 125.2, 120.1, 58.7, 42.6 ppm. IR (neat): ν = 3277, 3020, 2927, 1450, 1322, 1150, 1068, 979, 743 cm^{-1}. HRMS (ESI): calculated for $C_{14}H_{13}NO_2SNa$ $[M + Na]^+$ requires *m*/*z* 282.05647, found *m*/*z* 282.05969.

***N*-(2-Bromo-9*H*-fluoren-9-yl)-4-chlorobenzenesulfonamide (20).** Tan solid (17 mg, 16%). M.p. 197–200 °C. Purification (hexanes : EtOAc, 80 : 20). R_f = 0.45. ^{1}H NMR (400 MHz, $CDCl_3$): δ = 7.98 (dt, J_1 = 9.4 Hz, J_2 = 2.3 × (2) Hz, 2H), 7.60 (m, 3H), 7.48 (s, 2H), 7.37 (t, J_1 = 7.4 × (2) Hz, 1H), 7.27 (m, 2H), 7.18 (d, J_1 = 7.0 Hz, 1H), 5.38 (d, J_1 = 9.8 Hz, 1H), 4.87 (d, J_1 = 9.8 Hz, 1H) ppm. ^{13}C NMR (100 MHz, $CDCl_3$): δ 145.0, 142.5, 139.8, 139.7, 139.1, 139.0, 132.2, 129.8, 129.4, 128.7, 128.6, 128.4, 125.1, 121.7, 121.3, 120.2, 58.2 ppm. IR (neat): ν = 3272, 2922, 2852, 1435, 1336, 1159, 1065, 757 cm^{-1}. HRMS (ESI): calculated for $C_{19}H_{12}BrClNO_2S$ $[M - H]^+$ requires *m*/*z* 432.95389, found *m*/*z* 432.94989.

4-Chloro-*N*-(2-iodo-9*H*-fluoren-9-yl)benzenesulfonamide (21). White solid (7 mg, 6%). M.p. 220–222 °C. Purification (hexanes : EtOAc, 90 : 10). R_f = 0.14. ^{1}H NMR (400 MHz, $CDCl_3$): δ = 7.98 (dt, J_1 = 8.2 Hz, J_2 = 2.3 × (2) Hz, 2H), 7.68 (d, J_1 = 7.4 Hz, 1H), 7.61 (m, 3H), 7.37 (m, 3H), 7.29 (d, J_1 = 7.4 Hz, 1H), 7.20 (d, J_1 = 7.4 Hz, 1H), 5.38 (d, J_1 = 9.8 Hz, 1H), 4.83 (d, J_1 = 9.8 Hz, 1H) ppm. ^{13}C NMR (100 MHz, $CDCl_3$): δ 145.1, 142.3, 139.8, 139.6, 139.1, 138.1, 134.5, 129.9, 129.4, 128.7, 128.6, 125.1, 121.6, 120.2, 92.9, 58.2 ppm. IR (neat): ν = 3283, 1586, 1335, 1159, 1065, 772, 547 cm^{-1}. HRMS (ESI): calculated for $C_{19}H_{12}ClINO_2S$ $[M - H]^-$ requires *m*/*z* 479.93221, found *m*/*z* 479.92819.

4-Chloro-*N*-(9*H*-thioxanthen-9-yl)benzenesulfonamide (22). Performed on 0.125 mmol limiting reagent scale. Brown oil (32 mg, 66%). Purification (hexanes : EtOAc, 85 : 15). R_f = 0.03. ^{1}H NMR (400 MHz, $CDCl_3$): δ = 7.94 (dt, J_1 = 9.0 Hz, J_2 = 2.7 × (2) Hz, 2H), 7.74 (d, J_1 = 7.8 Hz, 2H), 7.45 (m, 8H), 4.36 (d, J_1 = 17.2 Hz, 1H), 3.92 (d, J_1 = 17.2 Hz, 1H) ppm. ^{13}C NMR (100 MHz, $CDCl_3$): δ 142.6, 137.7, 134.9, 132.1, 131.6, 129.0, 128.9, 128.1, 127.9, 126.4, 35.7 ppm. IR (neat): ν = 3057, 1709, 1145, 1088, 959, 731 cm^{-1}. HRMS (ESI): calculated for $C_{19}H_{15}ClNO_2S_2$ $[M + H]^+$ requires *m*/*z* 388.02328, found *m*/*z* 388.02399.

4-Methoxy-*N*-(9*H*-thioxanthen-9-yl)benzenesulfonamide (23).[32] Performed on 0.125 mmol limiting reagent scale. White oil (6.7 mg, 14%). Purification (hexanes : EtOAc, 50 : 50). ^{1}H NMR (400 MHz, $CDCl_3$): δ = 7.98 (dt, J_1 = 9.8 Hz, J_2 = 2.7 × (2) Hz, 2H), 7.79 (d, J_1 = 7.8 Hz, 2H), 7.45 (m, 6H), 6.96 (dt, J_1 = 9.8 Hz, J_2 = 2.7 × (2) Hz, 2H), 4.30 (d, J_1 = 17.2 Hz, 1H), 3.91 (d, J_1 = 17.2 Hz, 1H), 3.86 (s, 3H) ppm. ^{13}C NMR (100 MHz, $CDCl_3$): δ 162.0, 136.2, 134.3, 132.9, 131.3, 128.7, 128.4, 128.1, 126.2, 113.9, 55.5, 35.8 ppm. IR (neat): ν = 2928, 1595, 1497, 1289, 1256, 1142, 1088, 958, 755 cm^{-1}. HRMS (ESI): calculated for $C_{20}H_{18}NO_3S_2$ $[M + H]^+$ requires *m*/*z* 384.07281, found *m*/*z* 384.07327.

Conflicts of interest

There are no conflicts to declare.

Acknowledgements

The research results discussed in this publication were made possible in part by funding through the award for project number HR18-013, from the Oklahoma Center for the Advancement of Science and Technology. A. A. L. is grateful for the financial support provided by the lab start-up contribution from The University of Tulsa. We would also like to thank the Tulsa Undergraduate Research Challenge (TURC) and Chemistry Summer Undergraduate Research Program (CSURP) for support. Finally, we acknowledge the critical

insights and advice offered by Dr. Kenneth Roberts regarding the determination of log *P* values.

Notes and references

1 E. Tacconelli, E. Carrara, A. Savoldi, S. Harbarth, M. Mendelson, D. L. Monnet, C. Pulcini, G. Kahlmeter, J. Kluytmans, Y. Carmeli, M. Ouellette, K. Outterson, J. Patel, M. Cavaleri, E. M. Cox, C. R. Houchens, M. L. Grayson, P. Hansen, N. Singh, U. Theuretzbacher, N. Magrini, A. O. Aboderin, S. S. Al-Abri, N. Awang Jalil, N. Benzonana, S. Bhattacharya, A. J. Brink, F. R. Burkert, O. Cars, G. Cornaglia, O. J. Dyar, A. W. Friedrich, A. C. Gales, S. Gandra, C. G. Giske, D. A. Goff, H. Goossens, T. Gottlieb, M. Guzman Blanco, W. Hryniewicz, D. Kattula, T. Jinks, S. S. Kanj, L. Kerr, M.-P. Kieny, Y. S. Kim, R. S. Kozlov, J. Labarca, R. Laxminarayan, K. Leder, L. Leibovici, G. Levy-Hara, J. Littman, S. Malhotra-Kumar, V. Manchanda, L. Moja, B. Ndoye, A. Pan, D. L. Paterson, M. Paul, H. Qiu, P. Ramon-Pardo, J. Rodríguez-Baño, M. Sanguinetti, S. Sengupta, M. Sharland, M. Si-Mehand, L. L. Silver, W. Song, M. Steinbakk, J. Thomsen, G. E. Thwaites, J. W. M. van der Meer, N. Van Kinh, S. Vega, M. V. Villegas, A. Wechsler-Fördös, H. F. L. Wertheim, E. Wesangula, N. Woodford, F. O. Yilmaz and A. Zorzet, *Lancet Infect. Dis.*, 2018, **18**, 318–327.

2 (*a*) E. M. Eichenberger and J. T. Thaden, *Antibiotics*, 2019, **8**, 37; (*b*) R. Pereira da Cruz, T. Sampaio de Freitas, M. do Socorro Costa, A. T. Lucas Dos Santos, F. Ferreira Campina, R. L. S. Pereira, J. W. A. Bezerra, L. J. Quintans-Junior, A. A. De Souza Araujo, J. P. S. Junior, M. Iriti, E. M. Varoni, I. R. A. Menezes, H. D. Melo Coutinho and M. F. Bezerra Morais-Braga, *Antibiotics*, 2020, **9**, 28.

3 Y. Otsuka, *Chem. Pharm. Bull.*, 2020, **68**, 182–190.

4 A. Y. Gahane, P. Ranjan, V. Singh, R. K. Sharma, N. Sinha, M. Sharma, R. Chaudhry and A. K. Thakur, *Soft Matter*, 2018, **14**, 2234–2244.

5 For selected examples, see: (*a*) J. E. Anthony, *Chem. Rev.*, 2006, **106**, 5028–5048; (*b*) A. R. Murphy and J. M. J. Fréchet, *Chem. Rev.*, 2007, **107**, 1066–1096; (*c*) J. Wu, W. Pisula and K. Müllen, *Chem. Rev.*, 2007, **107**, 718–747; (*d*) O. InganÄs, F. Zhang and M. R. Andersson, *Acc. Chem. Res.*, 2009, **42**, 1731–1739; (*e*) J. Mei, Y. Diao, A. L. Appleton, L. Fang and Z. Bao, *J. Am. Chem. Soc.*, 2013, **135**, 6724–6746; (*f*) M. Ball, Y. Zhong, Y. Wu, C. Schenck, F. Ng, M. Steigerwald, S. Xiao and C. Nuckolls, *Acc. Chem. Res.*, 2015, **48**, 267–276; (*g*) W. Yang and W. A. Chalifoux, *Synlett*, 2017, **28**, 625–632.

6 (*a*) M. N. Soltani Rad, S. Behrouz, E. Zarenezhad, M. H. Moslemin, A. Zarenezhad, M. Mardkhoshnood, M. Behrouz and S. Rostami, *Med. Chem. Res.*, 2014, **23**, 3810–3822; (*b*) S. Ni, Y. Yuan, J. Huang, X. Mao, M. Lv, J. Zhu, X. Shen, J. Pei, L. Lai, H. Jiang and J. Li, *J. Med. Chem.*, 2009, **52**, 5295–5298; (*c*) A. Chollet, G. Mori, C. Menendez, F. Rodriguez, I. Fabing, M. R. Pasca, J. Madacki, J. Korduláková, P. Constant, A. Quémard, V. Bernardes-Génisson, C. Lherbet and M. Baltas, *Eur. J. Med. Chem.*, 2015, **101**, 218–235; (*d*) M. R. Kuo, H. R. Morbidoni, D. Alland, S. F. Sneddon, B. B. Gourlie, M. M. Staveski, M. Leonard, J. S. Gregory, A. D. Janjigian, C. Yee, J. M. Musser, B. Kreiswirth, H. Iwamoto, R. Perozzo, W. R. Jacobs Jr., J. C. Sacchettini and D. A. Fidock, *J. Biol. Chem.*, 2003, **278**, 20851–20859; (*e*) F. Vallée, C. Carrez, F. Pilorge, A. Dupuy, A. Parent, L. Bertin, F. Thompson, P. Ferrari, F. Fassy, A. Lamberton, A. Thomas, R. Arrebola, S. Guerif, A. Rohaut, V. Certal, J.-M. Ruxer, C. Delorme, A. Jouanen, J. Dumas, C. Grépin, C. Combeau, H. Goulaouic, N. Dereu, V. Mikol, P. Mailliet and H. Minoux, *J. Med. Chem.*, 2011, **54**, 7206–7219.

7 T. P. Stockdale and C. M. Williams, *Chem. Soc. Rev.*, 2015, **44**, 7737–7763.

8 A. C. Brueckner, E. N. Hancock, E. J. Anders, M. M. Tierney, H. R. Morgan, K. A. Scott and A. A. Lamar, *Org. Biomol. Chem.*, 2016, **14**, 4387–4392.

9 M. D. Hopkins, K. A. Scott, B. C. DeMier, H. R. Morgan, J. A. Macgruder and A. A. Lamar, *Org. Biomol. Chem.*, 2017, **15**, 9209–9216.

10 M. D. Hopkins, Z. C. Brandeburg, A. J. Hanson and A. A. Lamar, *Molecules*, 2018, **23**, 1838.

11 M. D. Hopkins, F. A. Abebe, K. A. Scott, G. L. Ozmer, A. A. Sheir, L. J. Schroeder, R. J. Sheaff and A. A. Lamar, *Org. Biomol. Chem.*, 2019, **17**, 8391–8402.

12 (*a*) N. A. Meanwell, *J. Med. Chem.*, 2011, **54**, 2529–2591; (*b*) C. Ballatore, D. M. Huryn and A. B. Smith, *ChemMedChem*, 2013, **8**, 385–395; (*c*) F. Minghao, T. Bingqing, H. L. Steven and J. Xuefeng, *Curr. Top. Med. Chem.*, 2016, **16**, 1200–1216; (*d*) F. Carta, A. Scozzafava and C. T. Supuran, *Expert Opin. Ther. Pat.*, 2012, **22**, 747–758; (*e*) A. K. Farhan, M. Sidra, N. Sadia, F. Umar, Z. Asma, S. M. Bukhari, R. Abdur and S. M. Mohammad, *Curr. Org. Chem.*, 2018, **22**, 818–830; (*f*) S. Apaydin and M. Torok, *Bioorg. Med. Chem. Lett.*, 2019, **29**, 2042–2050.

13 For representative examples, see: (*a*) X. Chen, S. Hussain, S. Parveen, S. Zhang, Y. Yang and C. Zhu, *Curr. Med. Chem.*, 2012, **19**, 3578–3604; (*b*) D. Patel, M. Jain, S. R. Shah, R. Bahekar, P. Jadav, A. Joharapurkar, N. Dhanesha, M. Shaikh, K. V. V. M. Sairam and P. Kapadnis, *Bioorg. Med. Chem. Lett.*, 2012, **22**, 1111–1117; (*c*) K. T. Andrews, G. M. Fisher, S. D. M. Sumanadasa, T. Skinner-Adams, J. Moeker, M. Lopez and S.-A. Poulsen, *Bioorg. Med. Chem. Lett.*, 2013, **23**, 6114–6117; (*d*) G. Chen, H. Ren, A. Turpoff, A. Arefolov, R. Wilde, J. Takasugi, A. Khan, N. Almstead, Z. Gu, T. Komatsu, C. Freund, J. Breslin, J. Colacino, J. Hedrick, M. Weetall and G. M. Karp, *Bioorg. Med. Chem. Lett.*, 2013, **23**, 3942–3946; (*e*) I. R. Greig, E. Coste, S. H. Ralston and R. J. van't Hof, *Bioorg. Med. Chem. Lett.*, 2013, **23**, 816–820; (*f*) T. Hanke, F. Rörsch, T. M. Thieme, N. Ferreiros, G. Schneider, G. Geisslinger, E. Proschak, S. Grösch and M. Schubert-Zsilavecz, *Bioorg. Med. Chem.*, 2013, **21**, 7874–7883; (*g*) S. Ovais, S. Yaseen, R. Bashir, P. Rathore, M. Samim, S. Singh, V. Nair and K. Javed, *J. Enzyme Inhib. Med. Chem.*, 2013, **28**, 1105–1112;

(*h*) A. Salahuddin, A. Inam, R. L. van Zyl, D. C. Heslop, C.-T. Chen, F. Avecilla, S. M. Agarwal and A. Azam, *Bioorg. Med. Chem.*, 2013, **21**, 3080–3089; (*i*) M. W. Carson, J. G. Luz, C. Suen, C. Montrose, R. Zink, X. Ruan, C. Cheng, H. Cole, M. D. Adrian, D. T. Kohlman, T. Mabry, N. Snyder, B. Condon, M. Maletic, D. Clawson, A. Pustilnik and M. J. Coghlan, *J. Med. Chem.*, 2014, **57**, 849–860; (*j*) T. A. Kirschberg, N. H. Squires, H. Yang, A. C. Corsa, Y. Tian, N. Tirunagari, X. C. Sheng and C. U. Kim, *Bioorg. Med. Chem. Lett.*, 2014, **24**, 969–972; (*k*) P. K. Ranjith, R. Pakkath, K. R. Haridas and S. N. Kumari, *Eur. J. Med. Chem.*, 2014, **71**, 354–365.

14 For selected examples of modern alternatives to sulfonamide formation, see: (*a*) D. L. Poeira, J. Macara, H. Faustino, J. A. S. Coelho, P. M. P. Gois and M. M. B. Marques, *Eur. J. Org. Chem.*, 2019, 2695–2701; (*b*) S. Caddick, J. D. Wilden and D. B. Judd, *J. Am. Chem. Soc.*, 2004, **126**, 1024–1025; (*c*) A. Shavnya, S. B. Coffey, A. C. Smith and V. Mascitti, *Org. Lett.*, 2013, **15**, 6226–6229; (*d*) A. S. Tsai, J. M. Curto, B. N. Rocke, A.-M. R. Dechert-Schmitt, G. K. Ingle and V. Mascitti, *Org. Lett.*, 2016, **18**, 508–511; (*e*) Y. Chen, P. R. D. Murray, A. T. Davies and M. C. Willis, *J. Am. Chem. Soc.*, 2018, **140**, 8781–8787; (*f*) A. S. Deeming, C. J. Russell and M. C. Willis, *Angew. Chem., Int. Ed.*, 2016, **55**, 747–750; (*g*) G. Laudadio, E. Barmpoutsis, C. Schotten, L. Struik, S. Govaerts, D. L. Browne and T. Noël, *J. Am. Chem. Soc.*, 2019, **141**, 5664–5668.

15 K. K. Anderson, *Comprehensive Organic Chemistry*, ed. D. N. Jones, Pergamon Press, Oxford, 1979, Vol. 3.

16 Y. Chen, *Synthesis*, 2016, **48**, 2483–2522 and references within. .

17 (*a*) X. Huang, J. Wang, Z. Ni, S. Wang and Y. Pan, *Chem. Commun.*, 2014, **50**, 4582–4584; (*b*) J. L. García Ruano, A. Parra, F. Yuste and V. M. Mastranzo, *Synthesis*, 2008, 311–319.

18 (*a*) X. Tang, L. Huang, C. Qi, X. Wu, W. Wu and H. Jiang, *Chem. Commun.*, 2013, **49**, 6102–6104; (*b*) C. Buathongjan, D. Beukeaw and S. Yotphan, *Eur. J. Org. Chem.*, 2015, 1575–1582; (*c*) J. Zhao, J. Xu, J. Chen, X. Wang and M. He, *RSC Adv.*, 2014, **4**, 64698–64701; (*d*) W. Wei, C. Liu, D. Yang, J. Wen, J. You and H. Wang, *Adv. Synth. Catal.*, 2015, **357**, 987–992.

19 For recent reviews, see: (*a*) S. Z. Zard, *Chem. Soc. Rev.*, 2008, **37**, 1603–1618; (*b*) S. B. Höfling and M. R. Heinrich, *Synthesis*, 2011, 173–189; (*c*) J.-R. Chen, X.-Q. Hu, L.-Q. Lu and W.-J. Xiao, *Chem. Soc. Rev.*, 2016, **45**, 2044–2056; (*d*) T. Xiong and Q. Zhang, *Chem. Soc. Rev.*, 2016, **45**, 3069–3087; (*e*) M. D. Kärkäs, *ACS Catal.*, 2017, **7**, 4999–5022; (*f*) Y. Zhao and W. Xia, *Chem. Soc. Rev.*, 2018, **47**, 2591–2608; (*g*) X.-Y. Yu, Q.-Q. Zhao, J. Chen, W.-J. Xiao and J.-R. Chen, *Acc. Chem. Res.*, 2020, **53**, 1066–1083.

20 (*a*) X. Yu and X. Lu, *Tetrahedron Lett.*, 2011, **52**, 2076–2079; (*b*) D. Huang, W. Yang, J. Zhang, X. Wang, X. Wang and Y. Hu, *RSC Adv.*, 2016, **6**, 47570–47578; (*c*) L. Chen, W. Teng, X.-L. Geng, Y.-F. Zhu, Y.-H. Guan and X. Fan, *Appl. Organomet. Chem.*, 2017, **31**, e3863; (*d*) X. Yu and X. Lu, *Adv. Synth. Catal.*, 2011, **353**, 569–574; (*e*) D. Huang, X. Wang, X. Wang, W. Chen, X. Wang and Y. Hu, *Org. Lett.*, 2016, **18**, 604–607.

21 (*a*) J. D. Harden, J. V. Ruppel, G. Y. Gao and X. P. Zhang, *Chem. Commun.*, 2007, 4644–4646, DOI: 10.1039/b710677g; (*b*) H. Baba and H. Togo, *Tetrahedron Lett.*, 2010, **51**, 2063–2066; (*c*) Y. Zhang, B. Feng and C. Zhu, *Org. Biomol. Chem.*, 2012, **10**, 9137–9141.

22 B. François, L. Szczubelek, F. Berrée, T. Roisnel and B. Carboni, *Adv. Synth. Catal.*, 2018, **360**, 235–241.

23 (*a*) V. Prasad, R. R. Kale, B. B. Mishra, D. Kumar and V. K. Tiwari, *Org. Lett.*, 2012, **14**, 2936–2939; (*b*) R. Fan, D. Pu, F. Wen and J. Wu, *J. Org. Chem.*, 2007, **72**, 8994–8997; (*c*) R. Fan, W. Li, D. Pu and L. Zhang, *Org. Lett.*, 2009, **11**, 1425–1428; (*d*) A. A. Lamar and K. M. Nicholas, *J. Org. Chem.*, 2010, **75**, 7644–7650.

24 R. Bedford, D. LePage, R. Hoffmann, S. Kennedy, T. Gutschenritter, L. Bull, N. Sujijantarat, J. C. DiCesare and R. J. Sheaff, *J. Photochem. Photobiol., B*, 2012, **107**, 55–64.

25 (*a*) J. M. Leitao and J. C. Esteves da Silva, *J. Photochem. Photobiol., B*, 2010, **101**, 1–8; (*b*) L. Miraglia, F. King and R. Damoiseaux, *Seeing the Light: Luminescent Reporter Gene Assays*, CCHTS, 2011; (*c*) L. H. Heitman, J. P. D. van Veldhoven, A. M. Zweemer, K. Ye, J. Brussee and A. P. Ijzerman, *J. Med. Chem.*, 2008, **51**, 4724–4729; (*d*) A. Braeuning, *Arch. Toxicol.*, 2015, **89**, 141–142.

26 For selected examples, see: (*a*) J. Gunter, R. H. Wenger and C. C. Scholz, *J. Photochem. Photobiol., B*, 2020, **210**, 111980; (*b*) Y. Liu, J. Fang, H. Cai, F. Xiao, K. Ding and Y. Hu, *Bioorg. Med. Chem.*, 2012, **20**, 5473–5482; (*c*) A. Braeuning and S. Vetter, *Biosci. Rep.*, 2012, **32**, 531–537; (*d*) B. Somanadhan, C. Leong, S. R. Whitton, S. Ng, A. D. Buss and M. S. Butler, *J. Nat. Prod.*, 2011, **74**, 1500–1502; (*e*) P. K. Poutiainen, J. J. Palvimo, A. E. Hinkkanen, A. Valkonen, T. K. Vaisanen, R. Laatikainen and J. T. Pulkkinen, *J. Med. Chem.*, 2013, **56**, 1064–1073; (*f*) I. V. L. Wilkinson, J. K. Reynolds, S. R. G. Galan, A. Vuorinen, A. J. Sills, E. Pires, G. M. Wynne, F. X. Wilson and A. J. Russell, *Bioorg. Chem.*, 2020, **94**, 103395; (*g*) H. Zhang, J. Su, Y. Lin, H. Bai, J. Liu, H. Chen, L. Du, L. Gu and M. Li, *Anal. Chem.*, 2017, **89**, 6099–6105; (*h*) H. Bai, P. Zhu, W. Wu, J. Li, Z. Ma, W. Zhang, Y. Cheng, L. Du and M. Li, *MedChemComm*, 2015, **6**, 418–424.

27 L. Peternel, M. Kotnik, A. Preželj and U. Urleb, *J. Biomol. Screening*, 2009, **14**, 142–150.

28 Organic Chemistry Portal: http://www.organic-chemistry.org/prog/peo/.

29 (*a*) A. Daina, O. Michielin and V. Zoete, *Sci. Rep.*, 2017, **7**, 42717; (*b*) http://www.swissadme.ch/.

30 A. Daina and V. Zoete, *ChemMedChem*, 2016, **11**, 1117–1121.

31 OECD, *Test No. 117: Partition Coefficient (n-octanol/water)*, HPLC Method, 2004.

32 T. Dohi, Y. Kita, K. Komiyama, S. Ueda and N. Yamaoka, *Heterocycles*, 2020, **100**, 85.

